Organic & Biomolecular Chemistry

Accepted Manuscript

ROYAL SOCIETY OF CHEMISTRY

www.rsc.org/obc

Mechanistic Insights into the Synergistic Catalysis by Au(I), Ga(III), and Counterions in Nakamura Reaction

*Rameswar Bhattacharjee, A. Nijamudheen, Ayan Datta**

Department of Spectroscopy, Indian Association for the Cultivation of Science, Jadavpur – 700032, West Bengal (India).

*Email: *spad@iacs.res.in*

Abstract

Computational study based on density functional theory (DFT) establishes the mechanisms for synergistic Au/Ga catalyzed addition of unactivated terminal alkynes to dicarbonyls, the Nakamura reaction. The role played by each of the metal catalysts and the counterion in the reaction has been elucidated. It has been shown that the triazole (TA) ligand could specifically activate the formation of a particular regioisomer through strong non-covalent interactions. Calculated regioselectivities and activation free energies are in excellent agreement with the experimental results. Observed regioselectivities were rationalized employing a distortion interaction analysis which suggests that the interaction between metal activated reactant fragments in the transition state geometries is a major factor that contributes to the overall barrier heights and selectivity. Such enhanced preference for the reaction at the alkyl/aryl substituted carbon of alkynes was strongly influenced by the additional non-covalent interactions exerted by the TA ligand. Excellent agreement between the calculations using homogeneous gold complex as the catalyst and experimentally observed kinetics and selectivity negates the role of *in situ* formed gold clusters in Nakamura reaction.

Keywords: *Nakamura reaction; Au(I) catalysis; DFT calculation; role of counterions; distortion – interaction model; qualitative molecular orbital theory (QMOT).*

Introduction

It is now rather well understood that the gold complexes being soft Lewis acids, can very efficiently catalyze a variety of C-C and C-X (X = N, O, S, and halides) coupling reactions through the π-philic activation of alkynes and olefins.[1] Plethora of reports have manifested their utility in the synthesis of natural products and other industrially important molecules with very good atom economy, while employing mild reaction conditions.[2] Recently, the synchronized use of gold complexes with other organic or organometallic catalysts has turned into a prominent synthetic strategy to achieve the desired selectivity and yield which was unattainable when any of these co-catalysts acted alone. For example, in the C-C cross coupling reactions, an external oxidative agent such as selectfluor is used to oxidize the Au(I) species to an Au(III) intermediate in the oxidative addition step.[3] Similarly, a meticulously chosen combination of a chiral Brønsted acid catalyst, an amine base, and a gold complex has been beneficial in enantioselective cooperative catalysis.[4]

Alternatively, one could think of a synergistic catalysis in which gold and a different metal/non-metal additive would simultaneously activate the nucleophile and electrophile respectively, in different catalytic cycles to realize one specific reaction.[5] In this context, a recent report by Shi and co-workers on the addition of 1,3-dicarbonyl compounds to unactivated terminal alkynes (also known as Nakamura reaction) catalyzed by the bimetallic synergistic catalysis of XPhosAu(TA)OTf and $Ga(OTf)_3$ complexes is particularly noteworthy.[6] The reaction occurred even with a very small quantity of gold catalysts (~500 ppm) at low temperature (45 °C) and it was proposed that Au(I) would activate the alkyne via a π-philic interaction whereas Ga(III) being a hard σ – Lewis acid, would enhance the acidity of 1,3-dicarbonyl compound via an oxophilic binding. It is interesting to note that all previously

reported mono-metallic catalysts based on In, Zn, Re, Ru, and Ir have required higher reaction temperatures to activate the Nakamura reaction.[7] Additionally, a number of other Au complexes and metal additives tested were found to be insufficient for this transformation.[6]

The present study was designed to gain insights into the following mechanistic aspects of this reaction; (a) The factors that control a delicate balance between XPhosAu(TA)OTf and $Ga(OTf)_3$ to form the best combination for the activation of Nakamura reaction. (b) Whether the Au(I) complex can activate the reaction or the *in situ* formed gold clusters which has been previously reported to occur in the C-I bond activation step in gold catalyzed Sonogashira reaction, drives the reaction.[8] (c) Role of ligands, as they are known to play pivotal roles in the realm of gold catalysis.[9] Recently developed triazole (TA) ligands with much improved thermal stability have been remarkable in activating a number of potential reactions.[10] However, to our knowledge, no experimental or computational studies have demonstrated the transition state (TS) models to depict the superior activity of TA ligands compared to other traditional ligands. (d) It is also intriguing to understand the significance of the counterion, OTf^- in the reaction mechanism especially because many recent computational studies have revealed the non-innocent roles of counterions in both reducing the activation barriers and deciding regioselectivity in multicomponent catalysis.[11] While there is a steady growth in the number of reports on cooperative gold catalyzed reactions, underpinning the mechanisms either by experiments or by theory have remained scarce.[12,13] Hence, a critical understanding of the pathways and the individual role of metal catalysts and ligands used in this novel and pertinent Au(I)/Ga(III) synergistic catalysis is important both in terms of fundamental chemistry involved and for further developments in the designing of potential catalysts for more complex reactions.

Here, our calculations based on DFT methods and TS modeling unravel the mechanisms for the Au/Ga catalyzed Nakamura reactions between dicarbonyls and terminal alkynes. The combined activation by Au/Ga catalysts is shown to create better frontier molecular orbital (FMO) energy matching between both reactants to promote the most plausible C-C bond forming path. The counterion OTf^- was found to play crucial roles in both proton abstraction and proto-demetalation steps. Excellent agreement was obtained between the experimentally observed regioselectivity and computationally predicted preferences in all cases. The observed trends in activation energies and selectivities could be rationalized based on distortion interaction model [14] and analysis of atomic charges of reactants.

Computational Methods and Models

DFT calculations were performed employing the hybrid M06-2X[15] functional using Gaussian 09.[16] This meta GGA functional incorporates medium range dispersion corrections and has been shown to be accurate for the calculation of thermochemistry and kinetics for organic and organometallic reactions and in the quantitative prediction of non covalent interactions.[17] All geometries were optimized using the standard 6-31G(d)[18] basis sets for the non-metal elements and LANL2DZ[19] basis sets consisting of a relativistic effective core (RECP) potential for the metals Au and Ga. This method has been represented as M06-2X/BS1 in the following sections for simplicity. At the same level of theory, harmonic vibrational frequencies were calculated to confirm whether the optimized structure is a ground state or a transition state geometry. The modes that correspond to unique imaginary frequency of each transition state were carefully verified and then intrinsic reaction coordinate (IRC)[20] calculations were carried out to ensure that the located TS do connect the correct reactants and products. Further, single point energies were computed at M06-2X/TZVP[21], LANL2TZ(f)[22] (for Au) level of theory which we represent as

M06-2X/BS2. Unless specified otherwise, all energies discussed were obtained at M06-2X/BS2//M06-2X/BS1 level incorporating zero point energy corrections calculated at M06-2X/BS1 level at 298.15 K. The significance of solvent effects were tested using an implicit polarizable continuum model (PCM) for chloroform (ε = 4.71) at IEFPCM[23]/M06-2X/BS2//M06-2X/BS1 level. To reduce the computational cost, calculation on the Au catalyst, $[XPhosAu(TA)]^+$ was performed by using a model system in which bulky cyclohexyl and isopropyl groups were replaced by CH_3 and H, respectively (see Scheme 1).[24] The effectiveness of such a model system on the energetics and regioselectivity was ascertained by the calculations performed with the actual catalyst.

Results and Discussion

***Scheme 1**: The Au/Ga catalyzed Nakamura reactions between terminal alkynes (**1**) and acetylacetone (**2**), and different Au(I) catalyst models used in the present study are shown.*

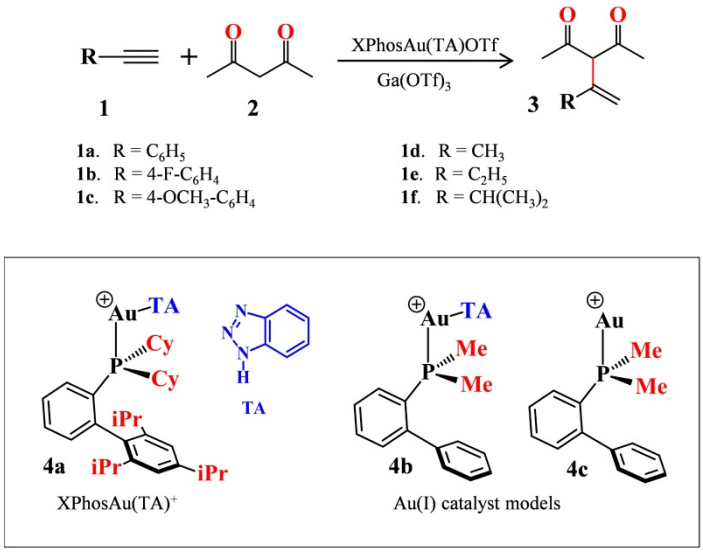

The terminal alkynes (**1**), acetylacetone (**2**) as the 1,3-dicarbonyl coupling partner, and the Au/Ga metal catalysts modeled to study the Nakamura reactions are depicted in Scheme 1. The

formation of a carbanion nucleophile from 1,3-dicarbonyl compound (**2**) is thermodynamically unfavorable in the absence of a Lewis acid because it is a strong base due to excess of negative charge building up at the carbon and oxygen sites. Along with this, the presence of a high-lying LUMO in **1** compared to the HOMO of **2** would make this reaction unviable. Calculations predict a LUMO energy of -0.21 eV for **1a** and HOMO energy of -8.9 eV for **2** leading to a large HOMO (**2)** – LUMO (**1a)** energy difference of 8.7 eV, which clearly explains the need of a catalyst to activate the reaction. Next, we studied the effect of Au/Ga catalysts in activating the FMO of **1a** and **1b**. Au catalyst (**4b**) would bind to the π – bond of **1b** in an unsymmetrical fashion with the Au – C bond distances of 2.49 and 2.33 Å (**9**, Figure 1). Upon binding with Au, the LUMO of **1a** gains significant stabilization as its energy changes from -0.2 eV in **1a** to -3.6 eV in **9**. Similarly, the activation of Ga with **2** through a Ga cycle (see Figure1) would generate its carbanion with a much higher HOMO level.

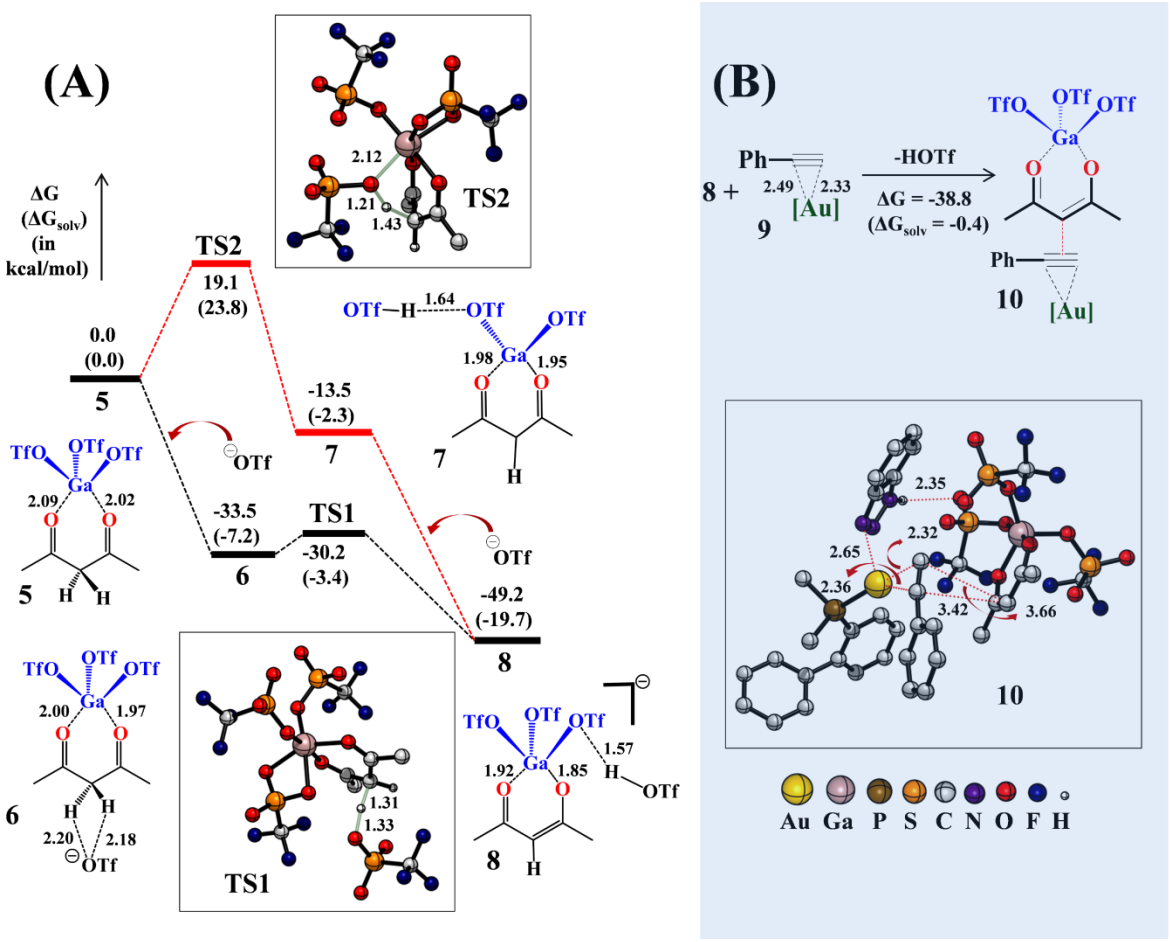

*Figure 1. (A) Gibb's free energy profiles computed for the Ga cycle depicting the mechanisms for the activation of **2** by Ga with the assistance of counterions. (B) The energetics for the formation of reactive intermediate complex (**10**) from the Ga activated dicarbonyl carbanion (**8**) and Au…alkyne piphilic complex (**9**). The free energy changes (in kcal/mol) obtained from both the gas phase (ΔG) and condensed phase (ΔG$_{solv}$) calculations and important bond distances (in Å) are given. Only selected H atoms are shown for better clarity.*

The feasibility of key steps involved in the Ga cycle could be envisioned from the computed free energy profile presented in Figure 1. In the initial step, the oxygen atoms in **1a** would coordinate with $Ga(OTf)_3$ to form the oxophilic complex **5**, which is stabilized by a BSSE corrected binding energy of -23.1 kcal/mol. Subsequently, **5** can undergo a deprotonation assisted by the counterion (OTf^-) either via an intramolecular or via an intermolecular pathway to generate the reactive carbanion nucleophile. For the energetically more favorable

intermolecular mechanism, a counterion from the solution would abstract the proton through the low energy transition state, **TS1** ($\Delta G^{\ddagger}$ = 3.3 kcal/mol) and large exergonicity (ΔG = -15.7 kcal/mol). From such favorable energetics (both low activation free energy and large exergonicity values), the formation of this enolate complex is predicted to be highly plausible. The alternate intramolecular proton abstraction mechanism by an OTf^{-} ion from $Ga(OTf)_3$ is unfavorable due to much higher activation free energy (19.1 kcal/mol) found for **TS2**. The intermediate **8** would then react with the Au…alkyne complex **9** to form the Au/Ga stabilized reactive intermediate **10** with the release of a molecule of HOTf. This reaction was identified to be energetically favorable by ΔG = -38.8 kcal/mol. **10** is stabilized due to two major non covalent interactions namely anion – π interactions between the π – bond of alkyne with the negatively charged carbanion (C…C distances of 3.42 Å and 3.66 Å) and an N-H…O hydrogen bond (of 2.35 Å) between the TA ligand and OTf ligand. Even though the incorporation of solvent effects leads to a smaller binding energy for **10**, it does not qualitatively change the proposed low energy pathways or any conclusions drawn from the gas phase calculations. Interestingly, the HOMO level in **8'** (**8** without the HOTf molecule) is substantially lifted to -6.0 eV from -8.9 eV calculated for **2**. As a result, a much smaller HOMO – LUMO gap (2.4 eV) was obtained between **8'** and **9** (see Figure 2). This FMO energy level matching could be a factor that promotes a low energy barrier for the C-C coupling in the presence of Au/Ga catalysts.

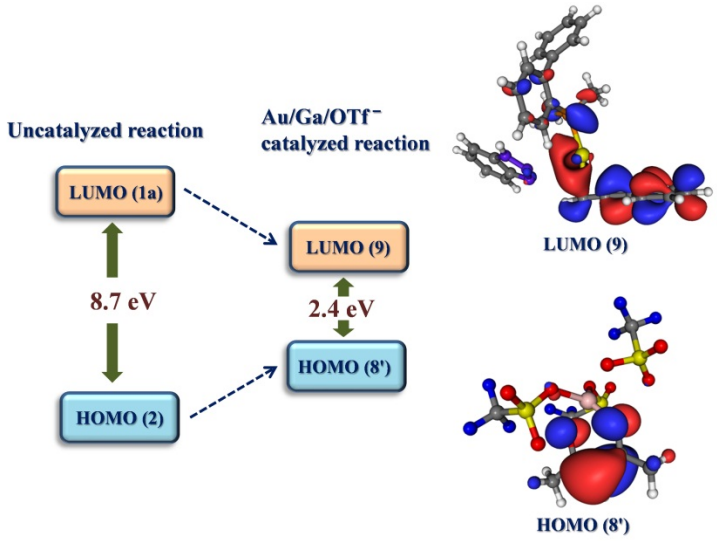

Figure 2: Synergistic activation of FMO by Au/Ga/OTf⁻ catalysts. Binding with Au stabilizes the LUMO level of ***1a*** *(in complex* ***9****) whereas the HUMO level for the Ga stabilized carbanion (complex* ***8'****) is higher than* ***2****. Corresponding FMO plots are also shown.*

The free energy profile calculated for the C-C coupling steps starting from **10** is shown in the Figure 3. This '*Au cycle*' would be initiated by the nucleophilic attack of dicarbonyl anion to the Au …alkyne moiety in an *anti* fashion to either of C_1 (-Ph substituted C) or C_2 (H substituted C) atoms. The possibility for the *syn* addition was excluded since the approach of the nucleophile in this fashion was *blocked* due to the steric hindrance by bulky ligands at Au center. Nevertheless, the preference for the anti addition of nucleophiles to Au…alkyne complexes to form a vinyl gold species is well documented in the literature except in some specific cases of norboranes[25]. The activation free energy calculated for the addition of dicarbonyl anion to C_1 to form the vinyl gold intermediate **11** is only 16.0 kcal/mol (for **TS3**). This reaction is slightly endergonic by 0.1 kcal/mol. The formation of this vinyl gold intermediate leads to the experimentally observed coupling product. Another possible reaction from the addition of the nucleophile at the C_2 position of the alkyne was ruled out due to a large barrier in **TS4** ($\Delta G^{\ddagger}$ =

20.9 kcal/mol). These results are in excellent agreement with the experimentally observed regioselectivity. Subsequently, the gold vinyl intermediate **11** would interact with an OTf^- counterion from the solvent to form the weakly bound complex **13**. Proto-demetalation step from **13** could regenerate the Au catalyst through a low energy barrier **TS5** ($\Delta G^{\ddagger}$ = 8.1 kcal/mol). Followed by this, the regeneration of Ga catalyst and the enolization of the coupling product would complete the catalytic cycle. Wang *et, al*. have shown that, for reactions in which protodeauration is the rate determining step, H-bonding interaction with the ligands like TA could be decisive.[12d] But, in the present work, such effects should be minimal as the regioselectivity determining step is the C-C bond formation step through the crossing of barrier, **TS3**. In the alternate pathway considered, the Ga catalyst would be regenerated from **11** before the proto-deauration step. However, this route was found to be higher in energy compared to the previous mechanism. In both cases, regeneration of the Ga catalyst was proposed to be occurring with the simultaneous activation of a new molecule of dicarbonyl reactant (**2**).

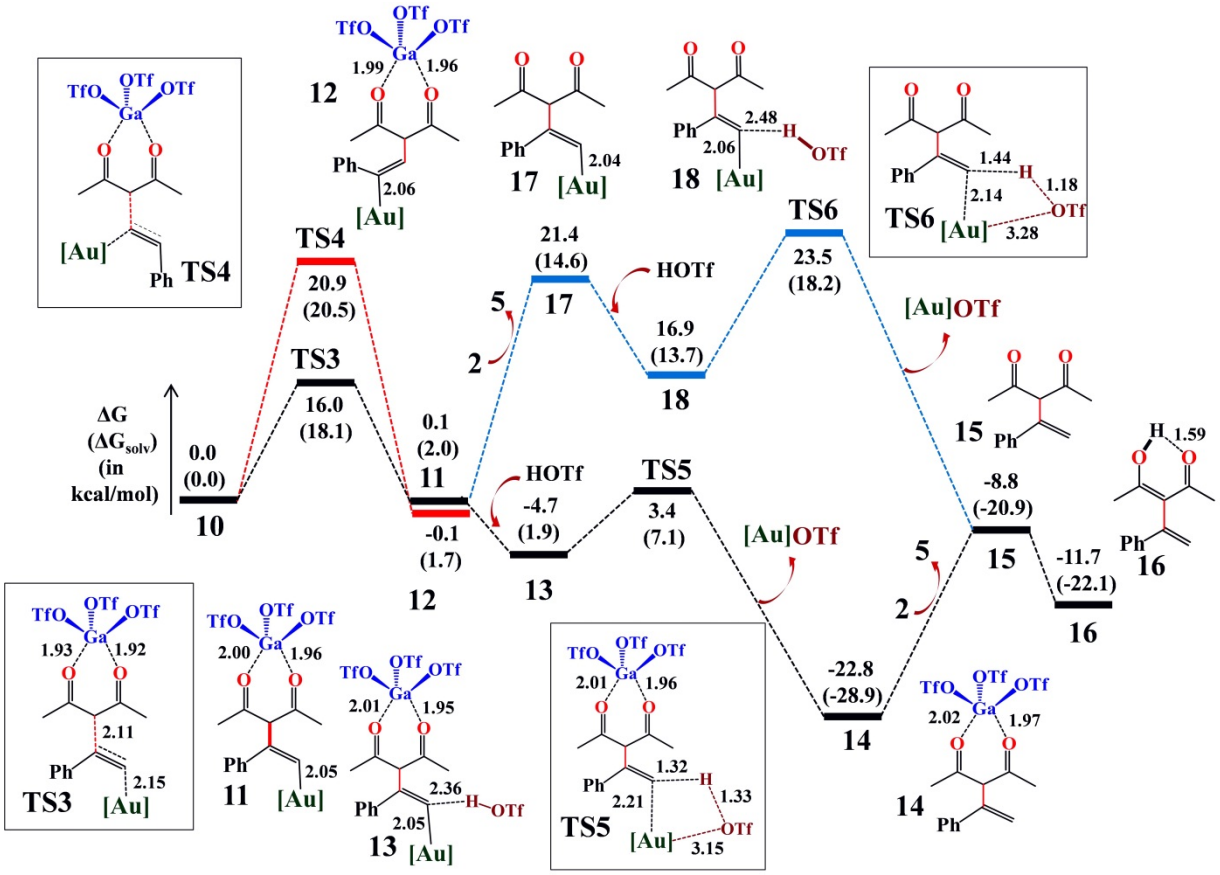

Figure 3. *Gibb's free energy profiles computed for the key steps involved in the Au cycle. The free energy changes (in kcal/mol) obtained from both the gas phase (ΔG) and condensed phase (ΔG$_{solv}$) calculations and important bond distances (in Å) are given.*

As it is evident from Figure 4, in the C-C coupling transition state (**TS3**), the predominant bonding interaction between TA ligand and Au is a weak metal…aromatic π type interaction (3.33 Å) whereas TA ligand forms a strong NH…O hydrogen bond (1.97 Å) with $Ga(OTf)_3$ moiety. Even though such Au…π(arene) interactions are not ubiquitous, they are known in the literature and have been recently reviewed by Caracelli and coworkers.[12d] Nevertheless, we have independently confirmed the presence of Au…π interactions instead of

Au…N interactions between Au and TA in **TS3** by performing relaxed IRC calculations between **10** and **11**. Additional calculations performed for the C-C bond forming step (**10** to **11**) using the model catalyst excluding TA from $[XPhos(TA)Au]^+$ predicted much higher activation energy of 21.1 kcal/mol. Importantly, the barrier for the attack at the less substituted C (C_2) was found to be similar for the calculations with or without the presence of TA ligand (20.5 kcal/mol for **TS8** in absence of TA compared to 20.9 kcal/mol for **TS4**). This shows that the TA ligand could stabilize one specific TS and thereby promoting a selective reaction compared to other possible reactions. Therefore, in addition to the enhanced thermal stability of Au(TA) complexes, the TA ligand could reduce the activation energy of the rate determining step and can control regeoselectivity through strong non-covalent interactions owing to its flexibility within the complex. In order to understand whether the involvement of Ga in the C-C bond making TS has any influence in the activation energy, this reaction was studied in the absence of Ga catalyst also. A very high activation energy was found for this TS in the absence of Ga catalyst ($\Delta\Delta G^{\ddagger}$ = 103.5 kcal/mol). Based on our findings, the most plausible mechanisms for the synergistic Au/Ga catalyzed addition of **1a** to **2** could be envisioned as shown in Scheme 2.

Scheme 2. Complete mechanism for the synergistic Au/Ga catalyzed C-C coupling between terminal alkynes and dicarbonyls.

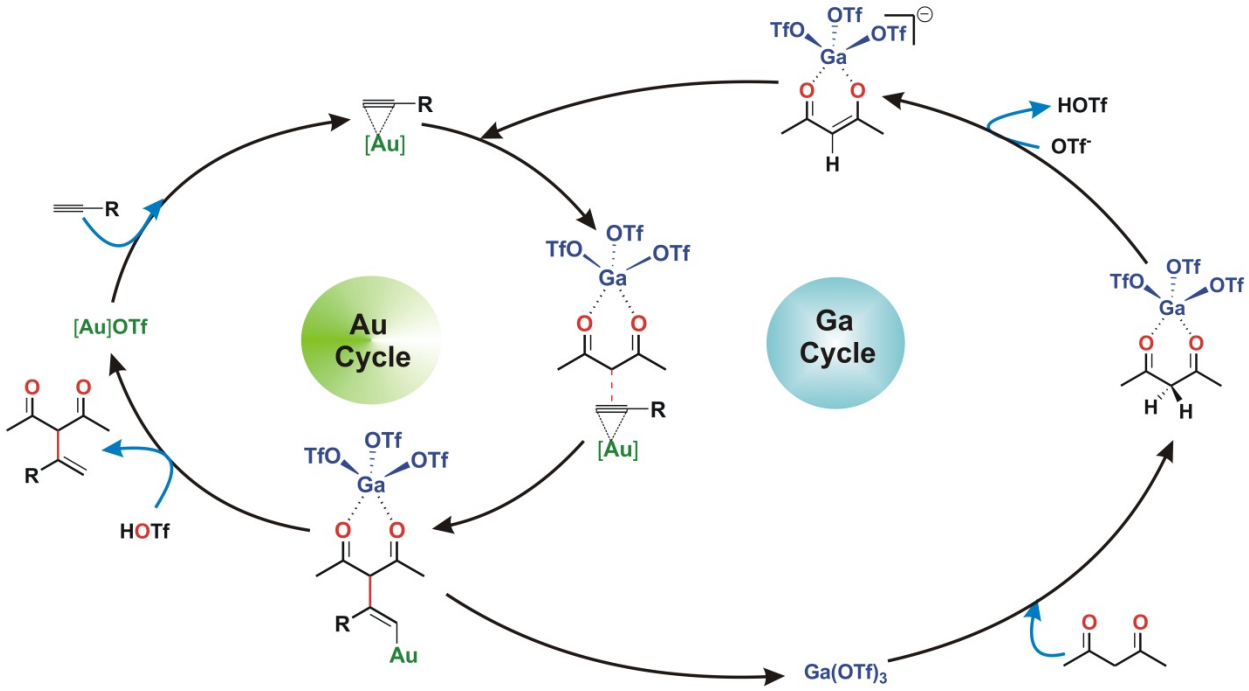

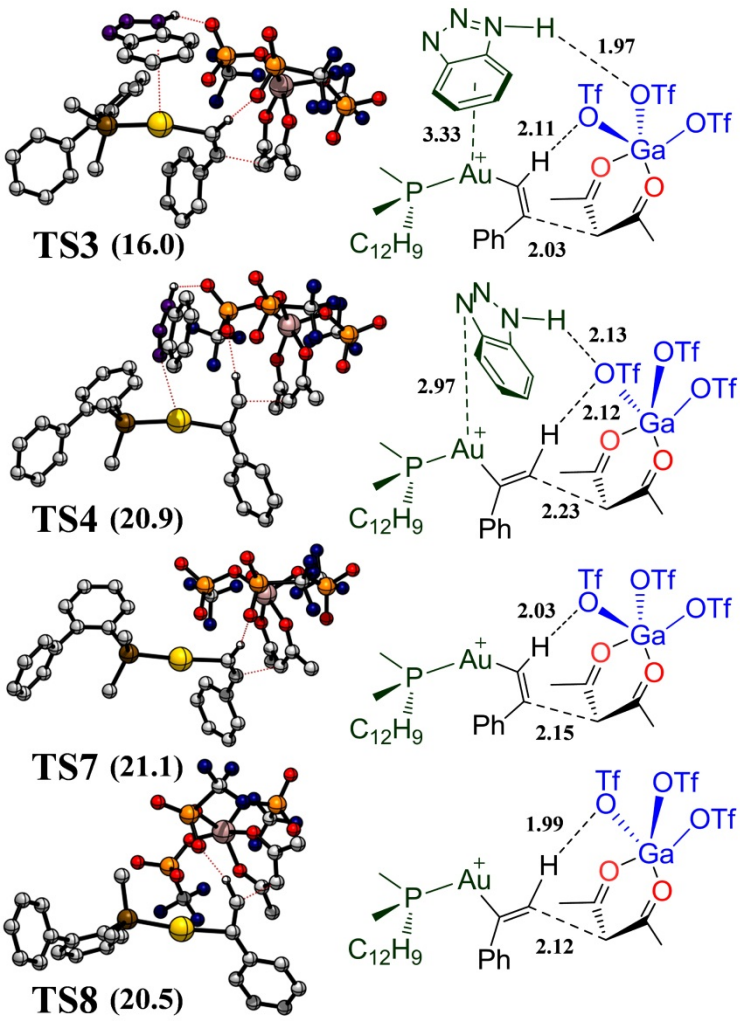

Figure 4. The geometries of C-C coupling transition states involved in the Au cycle optimized with and without TA ligand. Selected bond distances (in Å) and activation free energy (in kcal/mol) are shown. Only relevant H atoms are shown for improved clarity.

In order to gain a critical understanding on the regioselectivity of the reaction, we investigated the rate determining C-C coupling step for the Au/Ga catalyzed addition of **2** to a variety of terminal alkynes (**1a - 1f**, Table1). In all cases the nucleophilic addition to the more substituted end of the alkyne was found to be energetically favorable in agreement with that observed from the experimental studies. Significantly lower activation energies were found for the aryl substituted alkynes compared to the alkyl substituted ones. An analysis of the atomic

charges revealed that the hydrogen substituted carbon (C_2) is more negatively charged compared to C_1 and hence C_1 is more susceptible for the nucleophilic attack (See the Supporting Information file for the atomic charges from NBO calculations). The factors that contribute to the TS energy were quantified by employing a distortion – interaction model as shown in Figure 5 which is somewhat similar to the activation strain analysis proposed by Morokoma and suitably modified by Houk, Bickelhaupt, and coworkers for a variety of reactions[14]. Qualitatively, the distortion energies for π-philic Au complex of alkyne A or oxophilic Ga complex of dicarbonyl B (E_{dist} (A) or E_{dist} (B), respectively) in the TS are the energy required for A or B to distort from the respective ground state geometry to the TS geometry. Distortion energies were calculated as $E_{dist}(A) = E_A^{\ddagger} - E_A$ and $E_{dist}(B) = E_B^{\ddagger} - E_B$ where E_A (or E_B) and $E_A^{\ddagger}$ (or $E_B^{\ddagger}$) are the energies of A (or B) in ground state and transition state geometries, respectively. The interaction energies between A and B in the TS were also calculated by $E_{int} = \Delta E^{\ddagger} - E_{dist}$ - BE (AB) where $E_{dist} = E_{dist}(A) + E_{dist}(B)$, BE(AB) is the binding energy between A and B in the initial complex AB, and $\Delta E^{\ddagger}$ is the activation energy for the C-C coupling reaction. When considering the reactant complex AB as the reference, the activation energy could be written as $\Delta E^{\ddagger} = E_{dist}(eff) + E_{int}$ where $E_{dist}(eff) = E_{dist}$ - BE (AB) is the effective distortion energy. The distortion – interaction analysis relying on single point calculations at TS geometries were verified from additional calculations along the reaction coordinates also (see Supporting Information file).[14e]

As it is evident from the Table 1, the distortion energy corresponding to the Au-alkyne species (E_{dist} (A)) is substantially larger (21.8 - 28.1 kcal/mol) than the respective Ga-dicarbonyl species (E_{dist} (B), 5.9-7.3 kcal/mol), which is expected from the linear to angular structural transition of alkyne as going from the reactant to TS geometry. The magnitude of total distortion

energy (E_{dist} (eff)) strongly relates with the strength of the forming C-C bond in the transition state with a larger E_{dist} (eff) leads to short C-C bond and hence a later TS is predicted. Therefore, the E_{dist} (eff) for the coupling at C_1 was found to be larger compared to the coupling at C_2 (7.6 kcal/mol for **1a**). However, the most important contribution to the $\Delta E^{\ddagger}$ that decide the regioselectivity was found to be the interaction energy E_{int} between A and B in the TS. Therefore, **1a** (R = Ph) with a large difference in E_{int} for the coupling at C_1 compared to C_2 (ΔE_{int} = 13.3 kcal/mol) has clear preference for reaction at C_1 ($\Delta\Delta E^{\ddagger}$ = 5.7 kcal/mol). At the same time for **1d** (R = CH_3), E_{int} calculated for both TS corresponding to reaction at C_1 and C_2 were very similar ($\Delta\Delta E_{int}$ = 0.4 kcal/mol) and hence no selectivity was observed ($\Delta\Delta E^{\ddagger}$ = 0.1 kcal/mol). A linear relationship was obtained for a plot of $\Delta\Delta E_{int}$ against $\Delta\Delta E^{\ddagger}$ (see the Supporting Information).

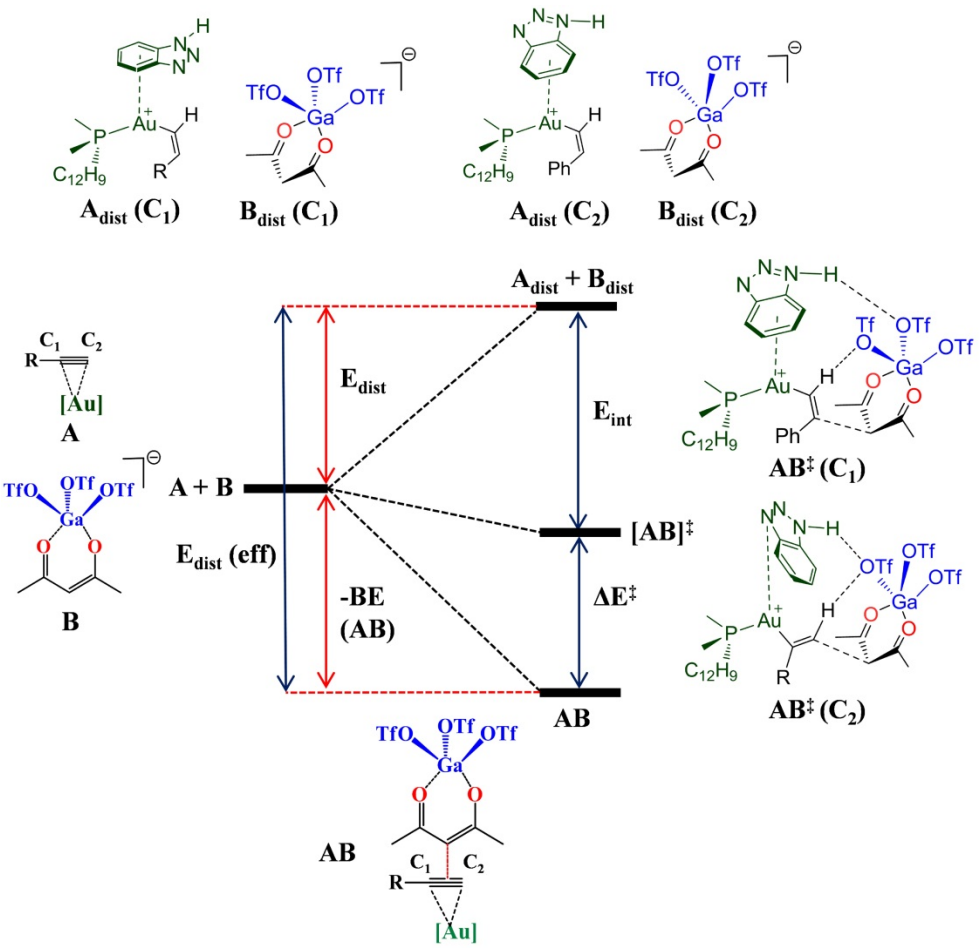

Figure 5. The scheme used to calculate the distortion and interaction energies between the Au-alkyne (A) and Ga-dicarbonyl (B) species.

*Table 1. The distortion and interaction energies calculated for the coupling of **2** with the alkynes **1a** – **1f**, **1a'**, and **1f'**.*

Alkyne coupling partner	Regio-selectivity (C_1/C_2)	$\Delta E^{\ddagger}$ (kcal/mol)	$\Delta G^{\ddagger}$ (kcal/mol)	BE of AB reactant complex (kcal/mol)	Distortion energy in TS (E_{dist}) (kcal/mol)				Interaction energy in TS ($E_{int} = \Delta E^{\ddagger} - E_{dist}$ (eff)) (kcal/mol)
					E_{dist} (A)	E_{dist} (B)	$E_{dist} = E_{dist}$ (A) + E_{dist} (B)	E_{dist} (eff) = E_{dist} - BE (AB) (kcal/mol)	
1a ($R = C_6H_5$)	C_1	13.5	16.0	-67.2	28.1	7.3	35.4	102.6	-89.1
	C_2	19.2	20.9		21.8	5.9	27.8	95.0	-75.8
1b ($R = 4\text{-F-}C_6H_4$)	C_1	12.7	16.4	-67.7	27.7	7.5	35.2	102.9	-90.1
	C_2	19.3	18.4		22.5	5.9	28.4	96.1	-76.8
1c ($R = 4\text{-OMe-}C_6H_4$)	C_1	12.6	15.1	-65.7	26.6	7.4	34.0	99.7	-87.1
	C_2	19.7	20.6		22.9	6.0	28.9	94.6	-74.9
1d ($R = CH_3$)	C_1	25.3	25.4	-70.9	22.2	6.4	28.6	99.5	-74.2
	C_2	25.0	24.5		22.3	6.4	28.7	99.6	-74.6
1e ($R = C_2H_5$)	C_1	17.5	18.3	-71.4	25.2	6.4	31.6	103.0	-85.5
	C_2	25.5	24.6		21.9	6.5	28.4	99.8	-74.3
1f ($R = CH(CH_3)_2$	C_1	19.5	21.5	-71.3	27.2	7.3	34.5	105.8	-86.3
	C_2	25.5	25.2		22.1	6.2	28.3	99.6	-74.5
1a' ($R = C_6H_5$, Au catalyst without TA ligand)	C_1	21.3	21.1	-72.4	18.6	6.90	25.5	97.9	-76.6
	C_2	20.5	20.5		24.9	7.0	31.9	104.3	-83.8
1f' ($R = CH(CH_3)_2$, Au catalyst without TA ligand)	C_1	30.2	28.9	-68.1	19.0	6.6	25.6	93.7	-73.1
	C_2	27.8	28.6		24.4	7.7	32.1	100.2	-82.0

The mode of action by which TA ligand selectively activate the C-C coupling at C_1 could be rationalized from a comparison of interaction energy (E_{int}) calculated for **1a** in the presence of Au catalyst with and without the TA ligand (**1a** and **1a'** in Table 1). In the absence of TA, E_{int} is significantly reduced for the coupling at C_1 (from -89.1 kcal/mol in **1a to** -76.6 kcal/mol in **1a'**) thereby leading to a large activation energy in the absence of TA. However, the absence of TA does not destabilize the TS for the coupling at C_2 of alkyne. These results further support the fact that TA reduces the activation energy through the noncovalent interactions in a specific TS.

Similarly, calculations to assess the role of TA were also performed for the reaction of an isopropyl substituted alkyne (**1f** and **1f'**, Table 1) and same conclusions were drawn.

Conclusions

In conclusion, mechanisms for the synergistic Au/Ga catalyzed addition of unactivated terminal alkynes to dicarbonyls were elucidated through DFT calculations. It has been shown that the simultaneous activation by metal catalysts would furnish FMO level matching between the two reactants to undergo an energetically favorable C-C bond forming reaction. The non-innocent role of counterions as a co-catalyst for both the proton abstraction and the protodemetalation steps were rationalized. While the present study establishes the role of OTf^- as crucial for this reaction, it would be interesting to study the role of other common counter anions such as F^-, Cl^-, Br^-, BF_4^-, OTs^-, TFA^-, and OAc^- instead OTf^- to gain a better understanding on the action of counter ion in the mechanism.[11] Calculations predict that apart from inducing enhanced thermal stability to the gold complexes, TA ligand could also significantly reduce the activation barrier for the reaction through strong non-covalent interaction and can control the regioselectivity of the reaction. The suggested mechanisms clearly demonstrate that the homogeneous gold complex used could efficiently activate the reaction and hence, the possibility of *in situ* gold cluster playing a role in the reaction is rather unlikely.

Computed regioselectivities for the Au/Ga catalyzed Nakamura reaction employing differently substituted terminal alkynes show very good agreement with the experimentally observed preference for the reaction. The origin for such selective C-C coupling reactions was unraveled by using a distortion – interaction model. In all cases, the calculated interaction energies between the metal activated reactants in the TS geometries were found to be a crucial

factor that controls the regioselectivity and overall activation energy of the reaction. The TA ligand could significantly increase the interaction energy of a specific TS structure thereby furnishing the regioselectivity of the reaction.

Acknowledgements

AD thanks to DST and INSA for partial funding. RB thanks CSIR for JRF.

Author Information

***Corresponding Authors: spad@iacs.res.in**

Notes

The authors declare no competing financial interest.

Supporting Information

Table S1, Fig S1-S4, Cartesian coordinates, electronic energies, zero–point energy correction to electronic energy (E_{ZPE}), zero–point energy correction to Gibb's free energies (G_{ZPE}) and zero–point energy corrected enthalpies (H_{ZPE}).

References:

1. (a) *Modern Gold Catalyzed Synthesis* (Eds.: A. S. K. Hashmi, F. D. Toste), Wiley-VCH, Weinheim, **2012** (b) Corma, A.; Leyva-Pérez, A.; Sabater, M. J. *Chem. Rev.* **2011**, *111*, 1657– 1712.
2. Selected recent reviews (a) Zhang, Y.; Luo, T.; Yang, Z. *Nat. Prod. Rep*. **2014**, *31*, 489. (b) Krause, N.; Winter, C. *Chem. Rev*. **2011**, *111*, 1994. (c) Rudolph, M.; Hashmi, A. S. K. *Chem. Soc. Rev*. **2012**, *41*, 2448.

3. (a) Stavber, S. *Molecules* **2011**, *16*, 6432. (b) Zhang, G.; Cui, L.; Wang, Y.; Zhang, L. *J. Am. Chem. Soc.* **2010**, *132*, 1474. (c) Ball, L. T.; Lloyd-Jones, G. C.; Russell, C. A. *Science* **2012**, *337*, 1644.

4. (a) Wang, Y-M.; Lackner, A. D.; Toste, D. F. *Acc. Chem. Res*. **2014**, *47*, 889. (b) Park, Y. J.; Park, J.-W.; Jun, C.-H. *Acc. Chem. Res.* **2008**, *41*, 222. (c) Wu, H.; He, Y.-P.; Gong, L.-Z. *Adv. Synth. Catal.* **2012**, *354*, 975. (d) Al-Amin, M.; Roth, K. E.; Blum, S. A. *ACS Catal.* **2014**, *4*, 622– 629.

5. (a) Allen, A. E.; MacMillan, D. W. C. *Chem. Sci.* **2012**, *3*, 633. (b) Breugst, M.; Grée, R.; Houk, K. N. *J. Org. Chem.* **2013**, *78*, 9892. (c) Skucas, E.; MacMillan, D. W. C. *J. Am. Chem. Soc.* **2012**, *134*, 9090. (d) Jiang, H.-L.; Akita, T.; Ishida, T.; Haruta, M.; Xu, Q. *J. Am. Chem. Soc.* **2011**, *133*, 1304.

6. Xi, Y.; Wang, D.; Ye, X.; Akhmedov, N. G.; Petersen, J. L.; Shi, X. *Org. Lett.* **2014**, *16*, 306.

7. (a) Nakamura, M.; Endo, K.; Nakamura, E. *J. Am. Chem. Soc.* **2003**, *125*, 13002. (b) Fujimoto, T.; Endo, K.; Tsuji, H.; Nakamura, M.; Nakamura, E. *J. Am. Chem. Soc.* **2008**, *130*, 4492. (c) Endo, K.; Hatakeyama, T.; Nakamura, M.; Nakamura, E. *J. Am. Chem. Soc.* **2007**, *129*, 5264. (d) Kennedy-Smith, J. J.; Staben, S. T.; Toste, F. D. *J. Am. Chem. Soc.* **2004**, *126*, 4526. (e) Kuninobu, Y.; Kawata, A.; Takai, K. *Org. Lett.* **2005**, *7*, 4823. (f) Tsuji, H.; Fujimoto, T.; Endo, K.; Nakamura, M.; Nakamura, E. *Org. Lett.* **2008**, *10*, 1219. (g) Onodera, G.; Kato, M.; Kawano, R.; Kometani, Y.; Takeuchi, R. *Org. Lett.* **2009**, *11*, 5038. (h) Murahashi, S.; Naota, T.; Nakano, Y. *Synlett.* **2009**, *20*, 3355. (i) Tsuji, H.; Tanaka, I.; Endo, K.; Yamagata, K.-i.; Nakamura, M.; Nakamura, E. *Org. Lett.* **2009**, *11*, 1845. (j) Cheung, H. W.; So, C. M.; Pun, K. H.; Zhou, Z.; Lau, C. P. *Adv.*

Synth. Catal. **2011**, *353,* 411. (k) Pennington-Boggio, M. K.; Conley, B. L.; Williams, T. J. J. *Organomet. Chem.* **2012**, *716*, 6.

8. (a) González-Arellano, C.; Abad, A.; Corma, A.; García, H.; Iglesias, M.; Sánchez, F. *Angew. Chem., Int. Ed*. **2007**, *46*, 1536. (b) Corma, A.; Juàrez, R.; Boronat, M.; Sànchez, F.; Iglesias, M.; García, H. *Chem. Commun*. **2011**, *47*, 1446. (c) Nijamudheen, A.; Datta, A, *J. Phys. Chem. C.* **2013**, *117*, 21433. (d) Boronat, M.; Combita, D.; Concepción, P.; Corma, A.; García, H.; Juárez, R.; Laursen, S.; De Dios López-Castro, *J. Phys. Chem. C* **2012**, *116*, 24855.
9. (a) Gorin, D. J.; Sherry, B. D.; Toste, F. D. *Chem. Rev.* **2008**, *108*, 3351.
10. (a) Duan, H.; Sengupta, S.; Petersen, J. L.; Akhmedov, N. G.; Shi, X. *J. Am. Chem. Soc.* **2009**, *131*, 12100. (b) Chen, Y.; Yan, W.; Akhmedov, N. G.; Shi, X. *Org. Lett.* **2009**, *12*, 344. (c) Wang, D.; Ye, X.; Shi, X. *Org. Lett*. **2010**, *12*, 2088. (d) Wang, D.; Gautam, L. N. S.; Bollinger, C.; Harris, A.; Li, M.; Shi, X. *Org. Lett.* **2011**, *13*, 2618. (e) Wang, Q.; Aparaj, S.; Akhmedov, N. G.; Petersen, J. L.; Shi, X. *Org. Lett.* **2012**, *14*, 1334.
11. (a) Jia, M.; Bandini, M. *ACS Cat*. **2015**, *5*, 1638. (b) Bandini, M.; Bottoni, A.; Chiarucci, M.; Cera, G.; Miscione, G. P. *J. Am. Chem. Soc*. **2012**, *134*, 20690. (c) Patil, N. T.; Nijamudheen, A.; Datta, A. *J. Org. Chem.* **2012**, *77*, 6179. (d) Ciancaleoni, G.; Belpassi, L.; Zuccaccia, D.; Tarantelli, F.; Belanzoni, P. *ACS Catal*. **2015**, *5*, 803. (e) Jindal, G.; Kisan, K. K.; Sunoj, B. *ACS Catal.,* **2015**, *5*, 480. (f) Sreenithya, A.; Sunoj, R. B. *Org. Lett*. **2014**, *16*, 6224.
12. (a) Wang, D.; Cai, R.; Sharma, S.; Jirak, J.; Thummanapelli, S. K.; Akhmedov, N. G.; Zhang, H.; Liu, X.; Petersen, J. L.; Shi, X. *J. Am. Chem. Soc.* **2012**, *134*, 9012. (b) Hashmi, A. S. K. *Acc. Chem. Res*. **2014**, *47*, 864. (c) Abbiati, G.; Rossi, E. *Beilstein J.*

Org. Chem. **2014**, *10*, 481. (d) Wang, W.; Kumar, M.; Hammond, G. B.; Xu, B. *Org. Lett*. **2014**, *16*, 636.

13. (a) Lv, H.; Zhan, J-H.; Cai, Y_B.; Yu, Y.; Wang, B.; Zhang, J-L. *J. Am. Chem. Soc*. **2012**, *134*, 16216. (b) Nijamudheen, A.; Jose, D.; Datta, A. *J. Phys. Chem. C*. **2011**, *115*, 2187. (c) Nijamudheen, A.; Karmakar, S. Datta, A. *Chem. Eur. J*. **2014,** *20*, 14650. (d) Cheong, P. H.; Morganelli, P.; Luzung, M. R.; Houk, K. N.; Toste, F. D. *J. Am. Chem. Soc*. **2008**, *130*, 4517.
14. (a) Kitaura, K.; Morokuma, K. *Int. J. Quant. Chem*. **1976**, *10*, 325 (b) Nagase, S. and Morokuma, K. *J. Am. Chem. Soc*. **1978**, *100*, 1666. (c) Bickelhaupt, F. M. *J. Comput. Chem*. **1999**, *20*, 114. (d) Diefenbach, A., de Jong, G. T., and Bickelhaupt, F. M. *Mol. Phys*. **2005**, *103*, 995. (e) van Zeist, W-J.; Bickelhaupt, F. M. *Org. Biomol. Chem*. **2010**, *8*, 3118. (f) Schoenebeck, F.; Houk, K. N. *J. Am. Chem. Soc.* **2010**, *132*, 2496. (g) Green, A. G.; Liu, P.; Merlic, C. A.; Houk, K. N. *J. Am. Chem. Soc.* **2014**, *136*, 4575.
15. Zhao, Y.; Truhlar, D. *Theor. Chem. Acc*. **2008**, *120*, 215.
16. Frisch, M. J.; Trucks, G. W.; Schlegel, H. B.; Scuseria, G. E.; Robb, M. A.; Cheeseman, J. R.; Scalmani, G.; Barone, V.; Mennucci, B.; Petersson, G. A.; Nakatsuji, H.; Caricato, M.; Li, X.; Hratchian, H. P.; Izmaylov, A. F.; Bloino, J.; Zheng, G.; Sonnenberg, J. L.; Hada, M.; Ehara, M.; Toyota, K.; Fukuda, R.; Hasegawa, J.; Ishida, M.; Nakajima, T.; Honda, Y.; Kitao, O.; Nakai, H.; Vreven, T.; Montgomery, Jr., J. A.; Peralta, J. E.; Ogliaro, F.; Bearpark, M.; Heyd, J. J.; Brothers, E.; Kudin, K. N.; Staroverov, V. N.; Kobayashi, R.; Normand, J.; Raghavachari, K.; Rendell, A.; Burant, J. C.; Iyengar, S. S.; Tomasi, J.; Cossi, M.; Rega, N.; Millam, J. M.; Klene, M.; Knox, J. E.; Cross, J. B.; Bakken, V.; Adamo, C.; Jaramillo, J.; Gomperts, R.; Stratmann, R. E.; Yazyev, O.;

Austin, A. J.; Cammi, R.; Pomelli, C.; Ochterski, J. W.; Martin, R. L.; Morokuma, K.; Zakrzewski, V. G.; Voth, G. A.; Salvador, P.; Dannenberg, J. J.; Dapprich, S.; Daniels, A. D.; Farkas, Ö.; Foresman, J. B.; Ortiz, J. V.; Cioslowski, J.; Fox, D. J. Gaussian 09, revision A.1; Gaussian, Inc.: Wallingford, CT, 2009.

17. (a) Zhao, Y.; Truhlar, D. G. *J. Chem. Theory Comput*. **2008**, *4*, 1849. (b) Nijamudheen, A.; Jose, D.; Shine, A.; Datta, A. *J. Phys. Chem. Lett*. **2012**, *3*, 1493. (c) Roy, S. R.; Nijamudheen, A.; Pariyar, A.; Ghosh, A.; Vardhanapu, P. K.; Mandal, P. K.; Datta, A.; Mandal, S. K. *ACS Cat*. **2014**, *4*, 4307. (d) Jissy, A. K.; Datta, A. *J. Phys. Chem. Lett.* **2013**, *4*, 1018. (e) Sun, Y. Y.; Chen, H. *J. Chem. Theory Comput.* **2013**, *9*, 4735. (f) Faza, O. N.; Rodríguez, R. Á.; López, S. C. *Theor. Chem. Acc.* **2011**, *128*, 647. (g) Laury, M. L.; Wilson, A. K. *J. Chem. Theory Comput.* **2013**, *9*, 3939. (h) Faza, O. N.; López, S. C. *Computational approaches to homogeneous gold catalysis* in *Top. Curr. Chem*. Springer, **2014**.
18. (a) Hehre, W. J.; Ditchfield, R.; Pople, J. A. *J. Chem. Phys.* **1972**, *56*, 2257. (b) Hariharan, P. C.; Pople, J. A. *Mol. Phys*. **1974**, *27*, 209.
19. Hay, P. J.; Wadt, W. R. *J. Chem. Phys.* **1985**, *82*, 299.
20. (a) Gonzalez, C.; Schlegel, H. B. *J. Chem. Phys*. **1989**, *90*, 2154. (b) Gonzalez, C.; Schlegel, H. B. *J. Phys. Chem.* **1990**, *94*, 5523.(c) Fukui, K. *Acct. Chem. Res.* **1981**, *14*, 363.
21. Dunning, T. H., Jr. *J. Chem. Phys*. **1971**, *55*, 716.
22. (a) Hay, P. J.; Wadt, W. R. *J. Chem. Phys*. **1985**, *82*, 299. (b) Ehlers, A. W.; Bohme, M.; Dapprich, S.; Gobbi, A.; Hollwarth, A.; Jonas, V.; Kohler, K. F.; Stegmann, R.; Veldkamp, A.; Frenking, G. *Chem. Phys. Lett.* **1993**, *208*, 111.

23. (a) Cancès, E.; Mennucci, B.; Tomasi, J. *J. Chem. Phys.* **1997**, *107*, 3032. (b) Mennucci, B.; Tomasi, J. *J. Chem. Phys.* **1997**, *106*, 5151. (c) Mennucci, B.; Cancès, E.; Tomasi, J. *J. Phys. Chem. B* **1997**, *101*, 10506. (d) Tomasi, J.; Mennucci, B.; Cancès, E. *J. Mol. Struct. (Theochem)* **1999**, *464*, 211.

24. Nevertheless, such a model for Au catalyst does not make any appreciable changes in the activation free energy as it was verified by performing calculations employing the actual catalyst (See Supporting Information).

25. (a) Cinellu, M. A.; Minghetti, G.; Cocco, F.; Stoccoro, S.; Zucca, A. *Angew. Chem.* **2005**, *117*, 7052. (b) Cinellu, M. A.; Minghetti, G.; Cocco, F.; Stoccoro, S.; Zucca, A. *Angew. Chem., Int. Ed.* **2005**, *44*, 6892.

26. Caracelli, I.; Zukerman-Schpector, J.; Tiekink, E. R. T. *Gold Bull*. **2013**, *46*, 81.

Graphical Table of Contents (TOC):

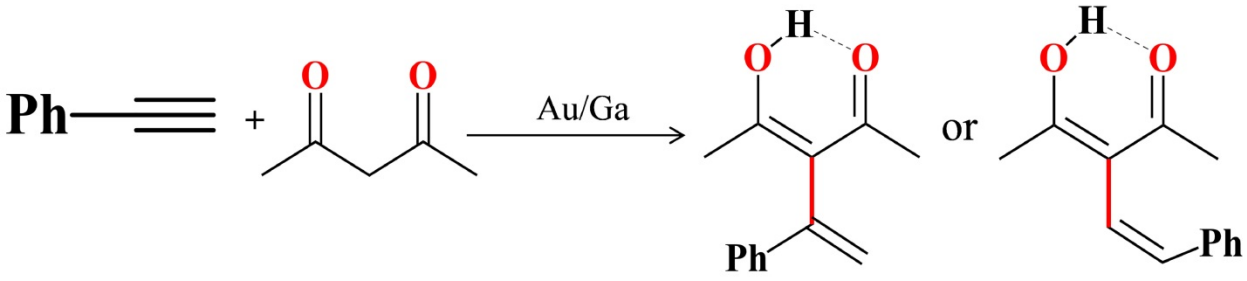

Au with TA ligand : Low Barrier and High Selectivity